Journal of Power Sources 196 (2011) 1694–1703

Contents lists available at ScienceDirect

Journal of Power Sources

journal homepage: www.elsevier.com/locate/jpowsour

Crosslinked sulfonated poly(arylene ether ketone) membranes bearing quinoxaline and acid–base complex cross-linkages for fuel cell applications

Xinbing Chen[a,*], Pei Chen[a], Zhongwei An[a], Kangcheng Chen[b], Kenichi Okamoto[b,**]

[a] Key Laboratory of Applied Surface and Colloid Chemistry, Ministry of Education, School of Chemistry and Materials Science, Shaanxi Normal University, Xi'an 710062, PR China
[b] Graduate School of Science and Engineering, Yamaguchi University, Tokiwadai 2-16-1, Ube, Yamaguchi 755-8611, Japan

ARTICLE INFO

Article history:
Received 1 September 2010
Received in revised form 12 October 2010
Accepted 14 October 2010
Available online 21 October 2010

Keywords:
Crosslinked sulfonated poly(arylene ether ketone)
Proton exchange membrane
Crosslinking
Methanol permeability
Proton conductivity

ABSTRACT

A series of crosslinkable sulfonated poly(arylene ether ketone)s (SPAEKs) were synthesized by copolymerization of 4,4′-biphenol with 2,6-difluorobenzil and 5,5′-carbonyl-bis(2-fluorobenzene-sulfonate). A facile crosslinking method was successfully developed, based on the cyclocondensation reaction of benzil moieties in polymer chain with 3,3′-diaminobenzidine to form quinoxaline groups acting as covalent and acid–base ionic crosslinking. The uncrosslinked and crosslinked SPAEK membranes showed high mechanical properties and the isotropic membrane swelling, while the later became insoluble in tested polar aprotic solvents. The crosslinking significantly improved the membrane performance, i.e., the crosslinked membranes had the lower membrane dimensional change, lower methanol permeability and higher oxidative stability than the corresponding precursor membranes, with keeping the reasonably high proton conductivity. The crosslinked membrane (**C-B4**) with an ion exchange capacity of 2.02 mequiv. g^{-1} showed a reasonably high proton conductivity of 111 mS cm^{-1} with a low water uptake of 42 wt% at 80 °C. **C-B4** exhibited a low methanol permeability of 0.55×10^{-6} cm^2 s^{-1} for 32 wt% methanol solution at 25 °C. The crosslinked SPAEK membranes have potential for PEFC and DMFC applications.

1. Introduction

In the past decades, as one of the most promising clean energy sources for transportation, stationary and portable power applications, polymer electrolyte membrane (PEM) fuel cells (PEFCs) and direct methanol fuel cells (DMFCs) have attracted considerable attentions due to their high efficiency and low pollution to environment. PEM is one of the key components in PEFC and DMFC systems, and serves as a proton conductor and a fuel separator between anode and cathode. Perfluorosulfonate polymer membranes such as DuPont's Nafion membranes are the state-of-art PEMs commercially available with features of high proton conductivity and excellent chemical stability [1,2]. However, large fuel crossover, lower operating temperature below 80 °C and high cost critically limit their widespread application [3]. Therefore, sulfonated aromatic polymers have been extensively studied as alternative PEMs [4–25].

Among alternative PEM materials, sulfonated poly(arylene ether)s (SPAEs) such as sulfonated poly(arylene ether sulfone)s (SPAESs) [13–19] and sulfonated poly(arylene ether ketone)s (SPAEKs) [20–22] are one of the promising candidates for fuel cell applications due to their good thermal and chemical stability. Proton conductivity and membrane stability are the most important properties determining the fuel cell applications. Generally, the proton conductivity significantly depends on the sulfonation level (or ion exchange capacity, IEC) and the water content sorbed in membrane. High proton conductivity can be achieved by controlling a relatively high sulfonation level (e.g. IEC > 2.0 mequiv. g^{-1}). Unfortunately, for SPAEs, such a high IEC makes them excessively swell and even soluble in water. Crosslinking is a common and powerful method to suppress membrane swelling and to improve the membrane durability. Kerres et al. reported ionically crosslinked acid/base blend membranes of SPAEK and polybenzimidazole (PBI) [26], and covalently crosslinked membranes via esterification reaction [27]. Kaliaguine and co-workers [28] and He and co-workers [29] developed a covalent crosslinking method based on a thermally activated reaction between poly(vinyl alcohol) and sulfonic acid groups in SPAEKs or sulfonated poly(phthalazinone ether sulfone ketone)s. Fang and co-workers [23(a),30] developed a facile crosslinking method with forming a stable sulfonyl group between sulfonic acid and electron-rich aromatic hydrogen. Another covalent crosslinking method via thermally or photochemically activated radical crosslinking reaction for SPAE membranes has been studied [31–33]. The covalent crosslinking methods are

* Corresponding author. Tel.: +86 029 85308081; fax: +86 029 85308090.
** Corresponding author. Tel.: +81 836 85 9660; fax: +81 836 85 9601.
E-mail addresses: chenxinbing@snnu.edu.cn (X. Chen), okamotok@yamaguchi-u.ac.jp (K. Okamoto).

0378-7753/$ – see front matter © 2010 Elsevier B.V. All rights reserved.
doi:10.1016/j.jpowsour.2010.10.039

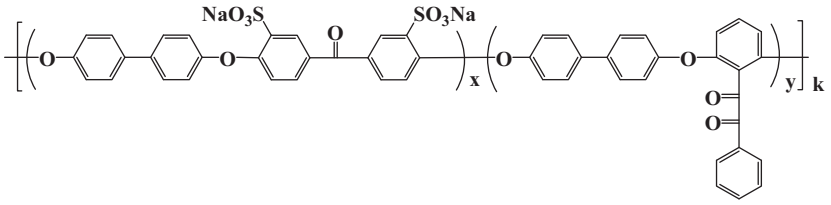

Scheme 1. Structure of crosslinkable sulfonated poly(arylene ether ketone) (SPAEK).

considered to be the most effective due to the formation of strong and stable crosslinking bonds.

In this paper, we have designed crosslinkable SPAEK copolymers bearing benzil moieties (Scheme 1), and developed a facile crosslinking method based on the cyclocondensation reaction of benzil moieties in polymer chains with 3,3′-diaminobenzidine to form quinoxaline groups, which act as covalent and acid–base ionic crosslinking. The properties including membrane swelling, proton conductivity, oxidative stability and methanol permeability for the crosslinked membranes have been investigated, compared with the corresponding precursor membranes.

2. Experimental

2.1. Materials

4,4′-Biphenol (BP) and 3,3′-diaminobenzidine (DAB) were purchased from Aladdin-reagent Co. and BP was purified by vacuum sublimation prior to use. 2,6-Difluorobenzonitrile and 4,4′-difluorobenzophenone were purchased from Aldrich and used as received. Dimethyl sulfoxide (DMSO), N,N-dimethylacetamide (DMAc), N,N-dimethylformamide (DMF) and 1-methyl-2-pyrrolidone (NMP) were purchased from Sinopharm Chemical Reagent Co. and dehydrated with molecular sieve 4A. Magnesium, absolute diethyl ether, benzyl chloride, copper (II) bromide, fuming sulfuric acid (20% SO_3), calcium hydride and other materials were purchased from Sinopharm Chemical Reagent Co. and used as received. NMP was dehydrated by calcium hydride, distilled under reduced pressure and then dried with molecular sieve 4A prior to use. 5,5′-Carbonyl-bis(2-fluorobenzene sulfonate) (CBFBS) was prepared by sulfonation of 4,4′-difluorobenzophenone at 120 °C using fuming sulfuric acid.

2.2. Synthesis

2,6-Difluorobenzil (DFB), nonsulfonated difluoride monomer, was prepared through two-step reactions, namely the nucleophilic addition of Grignard reagent to 2,6-difluorobenzonitrile followed by the oxidation, as shown in Scheme 2.

2.2.1. Synthesis of 1-(2,6-difluorophenyl)-2-phenyl-ethanone

The Grignard reagent of benzylmagnesium chloride was prepared by refluxing 0.14 mol of magnesium in 100 mL of absolute diethyl ether and 0.14 mol of benzyl chloride under N_2 atmosphere. To the solution of benzylmagnesium chloride in absolute diethyl ether, 0.14 mol of 2,6-difluorobenzonitrile in 100 mL of absolute diethyl ether was added slowly with stirring and refluxing under N_2 atmosphere. The reaction mixture was stirred under reflux for 6 h. The progress of the reaction was monitored by TLC. Then the reaction was quenched with 80 mL of 0.1 M hydrochloric acid, keeping the temperature below 25 °C. The ether layer was separated, and hydrolyzed in 200 mL of 1 M hydrochloric acid under reflux for 6 h. After hydrolysis, the ether layer was separated, washed with water to neutral, and dried over anhydrous sodium sulfate and concentrated under reduced pressure to yield oil. The oily product was distilled under reduced pressure, and the fraction of 1-(2,6-difluorophenyl)-2-phenyl-ethanone was collected at 100–105 °C/20 Pa with yield of 71%.

^{1}H NMR (300 MHz, $CDCl_3$, see Fig. 1(a)) δ(ppm): 4.16 (s, 2H, H6); 6.89 (t, J = 8.1 Hz, 2H, H2); 7.27 (m, 6H, H1 + H3 + H4 + H5). FT-IR (KBr, cm^{-1}): 3066, 3032, 2947, 2862 (CH_2), 1709, 1624 (C=O), 1596, 1466, 793, 702. MS m/z (rel. int.): 232 (M^+, <0.5%), 182 (25%), 104 (4%), 92 (11%), 91 (100%), 77 (4%), 65 (19%), 51 (4%).

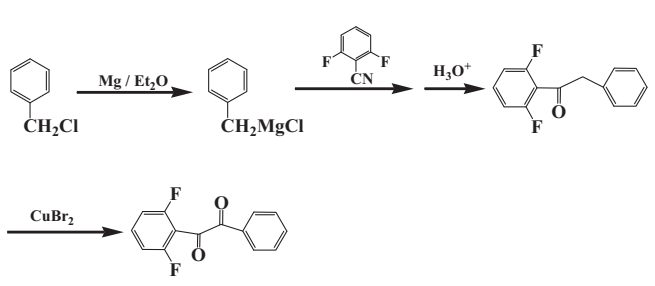

Scheme 2. Synthesis of 2,6-difluorobenzil (DFB).

2.2.2. Synthesis of DFB

To a 500 mL, three-neck, round-bottom flask equipped with an overhead stirrer and condenser, 16 g of 1-(2,6-difluorophenyl)-2-phenyl-ethanone (68.9 mmol), 32 g of $CuBr_2$ (143.3 mmol), 80 mL of DMSO, and 80 mL of ethyl acetate were added. The mixture was stirred under reflux overnight. After the mixture was cooled to room temperature, it was transferred to a separatory funnel with 150 mL of CH_2Cl_2. The organic layer was washed several times with water. The organic phase was filtered through Celite to remove insoluble copper salts. The filtrate was evaporated under reduced pressure to yield a yellow-green solid. The solid residue was recrystallized from ethanol. Yield 11.9 g (70%) of crystal (melting point: 104–105 °C). ^{1}H NMR (300 MHz, $CDCl_3$, see Fig. 1(b)) δ(ppm): 7.01 (t, J = 8.4 Hz, 2H, H2); 7.55 (m, 3H, H4 + H5); 7.69 (m, 1H, H1); 8.04 (d, J = 7.2 Hz, 2H, H3). FT-IR (KBr, cm^{-1}): 3103, 3070, 1693, 1626 (C=O), 1596, 1471, 694, 721. MS m/z (rel. int.): 246 (M^+, 1%), 141 (13%), 105 (100%), 77 (55%), 51 (17%).

2.2.3. Polymerization

SPAEK copolymer BP-CBFBS/DFB (x/y), where the data in parenthesis refer to the molar ratio of sulfonated difluoride monomer (CBFBS) to nonsulfonated one (DFB), was prepared by a one-pot high temperature polymerization method, as shown in Scheme 3. As an example, the preparation procedure of BP-CBFBS/DFB (1/1), **B4** in Table 1, is described below, To a 100 mL dry three-neck flask equipped with a Dean-Stark trap and a condenser, 2.111 g (5.0 mmol) of CBFBS, 1.230 g (5.0 mmol) of DFB, 1.862 g (10.0 mmol) of BP, 1.588 g (11.5 mmol) of anhydrous potassium carbonate, 26 mL of NMP and 15 mL of toluene were added under nitrogen flow with stirring. The reaction mixture was heated to 140 °C. Water and toluene were evaporated as the azeotrope and collected in the Dean-Stark trap. After water was completely evaporated (the Dean-Stark trap became clear), the reaction temperature was raised to 160 °C and the polymerization was continued at this temper-

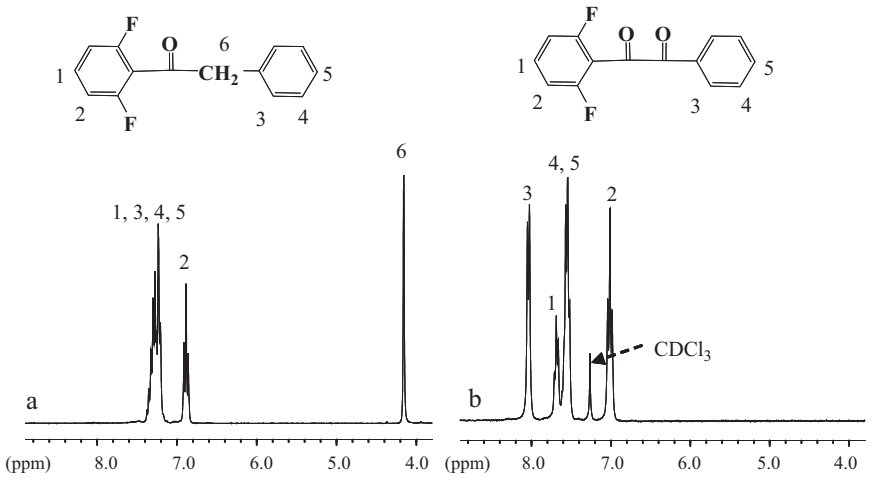

Fig. 1. ^{1}H NMR spectra of 1-(2,6-difluorophenyl)-2-phenyl-ethanone (a) and DFB (b) in $CDCl_3$.

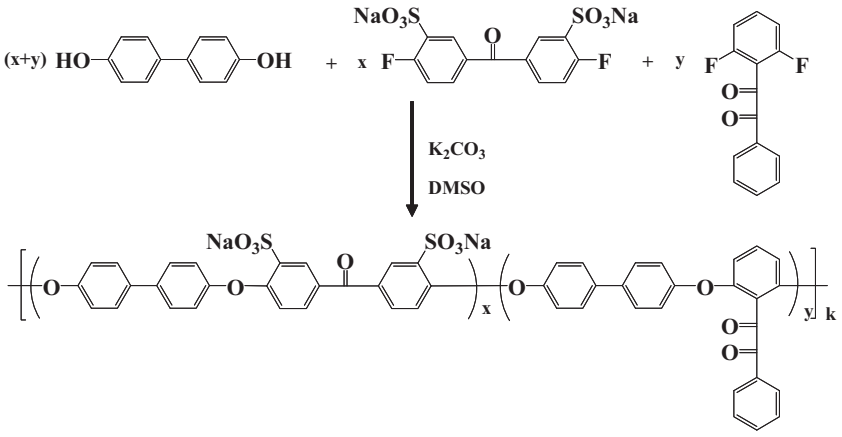

Scheme 3. Synthesis of crosslinkable SPAEK.

ature for 10 h. The resulting highly viscous solution was slowly poured into water. The resulting fiber-like precipitate was thoroughly washed in water with stirring at 80 °C overnight, and then washed with methanol, and dried at 120 °C in vacuum.

2.3. Membrane formation and proton exchange

2.3.1. Uncrosslinked SPAEK membrane

A 7 wt% SPAEK solution in DMSO was prepared and filtrated. The filtrate was cast onto glass plates at 80 °C, and dried at 100 °C for 12 h. The as-cast membranes were soaked in water at 40 °C for 48 h, and proton-exchanged with 1 M hydrochloric acid at 50 °C for 48 h. The proton-exchanged membranes were thoroughly washed with deionized water till the rinsed water became neutral, followed by drying in vacuum at 120 °C for 15 h. The membranes obtained were 40–60 μm in thickness.

2.3.2. Crosslinked SPAEK membrane

Crosslinked SPAEK membrane, BP-CBFBS/DFB/DAB (*x*/*y*/*z*), where the data in parenthesis (*x*/*y*/*z*) refer to the molar ratio of CBFBS:DFB:DAB, was prepared using the cyclocondensation reaction of benzil groups in DFB moieties and 3,3′-diaminobenzidine

Table 1
Basic properties of SPAEK membranes[a]

Code	SPAEK membrane	η_{int}[b] (dL g^{-1})	IEC[c] (mequiv. g^{-1})	WU (%)		λ		Size change[d]		$\Delta_{t/l}$[d]
				25 °C	80 °C	25 °C	80 °C	Δt_c	Δl_c	
B1	BP-CBFBS/DFB (4/1)	1.8	3.00(2.74)	175	260	32	48	0.60	0.63	0.95
C-B1	BP-CBFBS/DFB/DAB (4/1/0.5)	–	2.92(2.41)	114	185	22	35	0.41	0.43	0.96
B2	BP-CBFBS/DFB (2/1)	1.6	2.61(2.35)	90	158	19	34	0.46	0.44	1.03
C-B2	BP-CBFBS/DFB/DAB (2/1/0.3)	–	2.54(2.05)	60	92	13	20	0.29	0.30	0.95
B3	BP-CBFBS/DFB (3/2)	1.5	2.41(2.17)	75	131	17	30	0.35	0.34	1.05
C-B3	BP-CBFBS/DFB/DAB (3/2/0.5)	–	2.34(1.92)	52	77	12	18	0.21	0.22	0.96
B4	BP-CBFBS/DFB (1/1)	1.5	2.08(1.89)	42	63	11	17	0.21	0.21	1.00
C-B4	BP-CBFBS/DFB/DAB (1/1/0.2)	–	2.02(1.65)	31	42	9	12	0.11	0.11	0.98

[a] The experimental errors for IEC, WU and size change were ±1%, ±2% and ±3%, respectively.
[b] In DMSO solution at 35 °C.
[c] Calculated value; the data in parentheses are obtained by a titration method.
[d] At 80 °C.

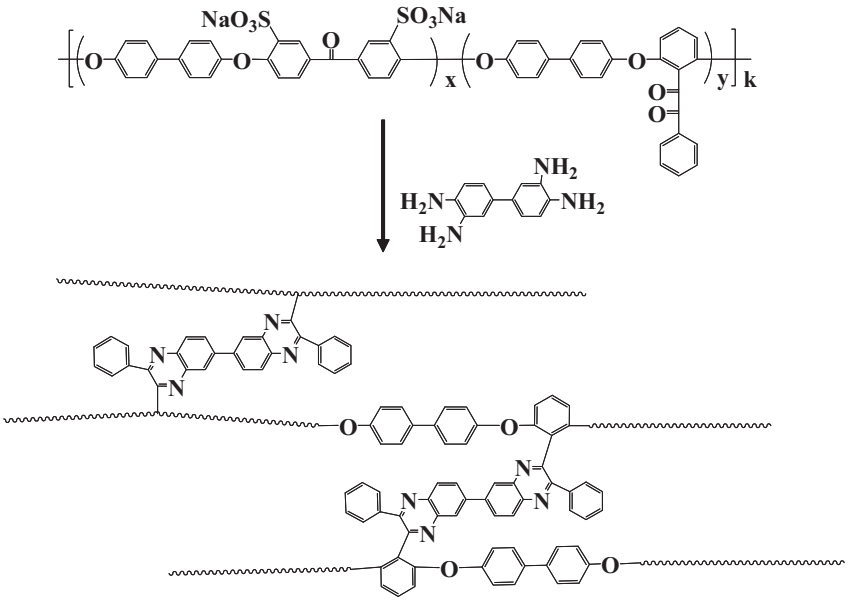

Scheme 4. Preparation of crosslinked SPAEK membrane.

(DAB) to form quinoxaline, as shown in Scheme 4. Here, the molar content of DAB was set as 10 mol% based on BP for all the crosslinked membranes, that is, $z = 0.1(x+y)$. As an example, the crosslinked membrane of BP-CBFBS/DFB/DAB (1/1/0.2), **C-B4** in Table 1, is described below.

A 7 wt% BP-CBFBS/DFB (1/1) solution in DMSO was prepared and filtrated. A given amount of DAB was added into the filtrate and the mixture was stirred at 140 °C for 4 h and then 160 °C for 3–3.5 h (the gelation took place if the reaction was continued for a longer time). The mixture was cooled and cast onto glass plates at 80 °C, and dried at 100 °C for 4 h, 120 °C for 2 h and then cured at 180 °C in vacuum for 5 h to promote the crosslinking reaction. The as-cast membranes were post-treated as mentioned above.

2.4. Characterization and measurements

FT-IR spectra were recorded on a Bruker Equinox 55 spectrometer. ^{1}H NMR spectra were recorded on a Bruker AV 300 (300 MHz) instrument. The mass spectra were obtained by GC/MS Thermo DSQ II with m/z 50–650. Thermogravimetric analysis (TGA) was carried out with a TA 600SDT in helium (flow rate: 100 cm^3 min^{-1}) at a heating rate of 10 °C min^{-1}, standing at 150 °C for 0.5 h. Mechanical tensile tests were performed on a universal testing machine (Orientic, Tensilon TRC-1150A) at 25 °C and about 70%RH at a crosshead speed of 5 mm min^{-1}. Solubility tests were carried out in DMAc, DMF, NMP, and DMSO with a concentration of 5% (w/v) at room temperature. The intrinsic viscosity (η_{int}) was measured with an Ubbelohde viscometer using DMSO solutions of SPAEK (concentrations of 0.55, 0.35 and 0.25 g dL^{-1}) at 35 °C.

Ion exchange capacity (IEC) was calculated from the molar ratio of sulfonated difluoride monomer to nonsulfonated one in feed, and also evaluated by a titration method. A sample membrane in proton form was soaked in a 15 wt% NaCl solution at 40 °C for 72 h and the released proton was titrated with a 0.05 M NaOH solution, using phenolphthalein as an indicator. The titration was carried out for the solutions containing the sample membranes within a few minutes.

Water uptake (WU) of membrane was obtained by calculating the weight difference between the dry and wet membranes. The completely dried membrane samples were weighed and then soaked into deionized water until the weight remained constant. Then the samples were taken out, wiped with tissue paper, and quickly weighted on a microbalance. The WU was calculated, using the following equation:

$$\mathrm{WU} = \frac{W_s - W_d}{W_d} \times 100\% \quad (1)$$

where W_s and W_d are the weights of swollen and dry membranes, respectively.

Dimensional change of membrane was measured by soaking more than two sample sheets in water at different temperatures. The *through-plane* and *in-plane* dimensional changes (Δt_c and Δl_c) and the membrane swelling ratio ($\Delta_{t/l}$) were calculated from Eq. (2):

$$\Delta t_c = \frac{t - t_d}{t_d} \times 100\%$$
$$\Delta l_c = \frac{l - l_d}{l_d} \times 100\% \quad (2)$$
$$\Delta_{t/l} = \frac{\Delta t_c}{\Delta l_c}$$

where t_d and l_d are the thickness and length of the dry membrane, respectively; t and l refer to those of the membrane immersed in water.

Proton conductivity of membrane was determined using an electrochemical impedance spectroscopy technique over the frequency from 100 Hz to 100 KHz (Hioki 3532-80). A single cell with two platinum plate electrodes was mounted on a Teflon plate at 0.5 cm distance. A membrane swollen in water at 25 °C was set in the cell. The cell was placed in deionized water. Proton conductivity was calculated from Eq. (3):

$$\sigma = \frac{d}{t_s w_s R} \quad (3)$$

where d is the distance (or membrane length) between the two electrodes, t_s and w_s are the thickness and width of the membrane in deionized water, respectively. The d, t_s and w_s values at different temperatures were evaluated from the temperature dependence of dimensional change of membrane.

Oxidative stability was determined using Fenton's reagent (3 wt% H_2O_2 + 2 ppm $FeSO_4$) at 80 °C. The membranes (50–60 μm in thickness) were immersed in Erlenmeyer flasks containing Fen-

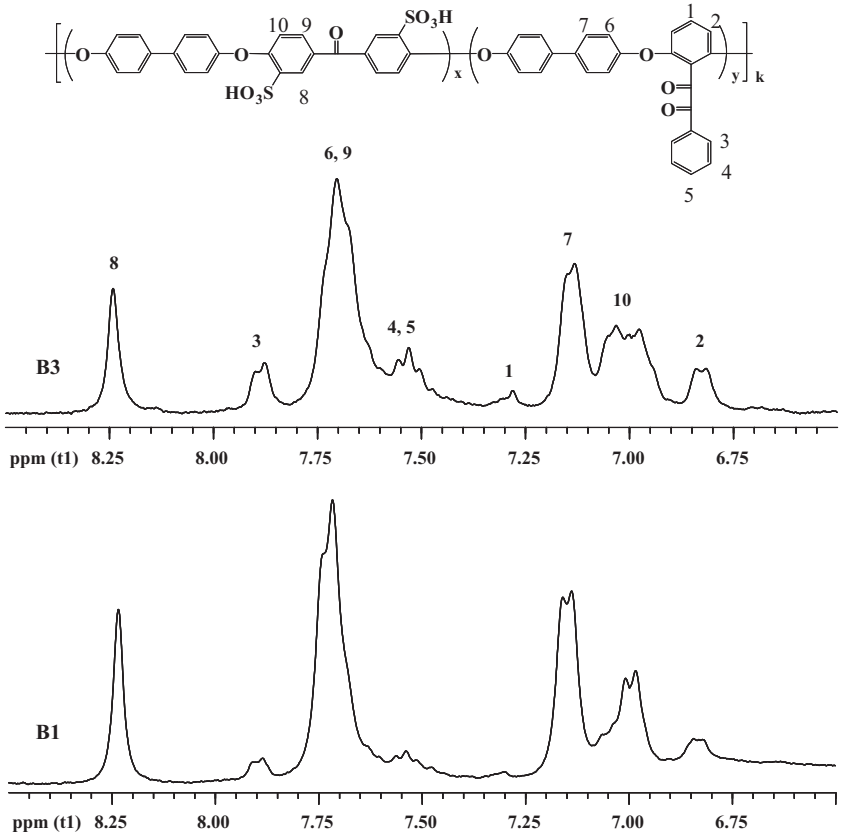

Fig. 2. ^{1}H NMR spectra of SPAEKs (**B1** and **B3**) in proton form in DMSO-d_6.

ton's reagent. The flasks were shaken vigorously once every 10 min until the membranes begin to break.

Methanol permeability (P_M) measurement was carried out using a liquid permeation cell composed of two compartments, which were separated by a vertical membrane. The membrane was first immersed in water for 2 h to get the water-swollen sample and then set into the measurement cell (effective area: 16 cm^2). One compartment of the cell (V_a = 400 mL) was filled with 32 wt% methanol feed solution, and the other compartment (V_b = 90 mL) was filled with deionized water. The compartments were stirred continuously during the permeability measurement. The methanol concentrations of the two compartments were analyzed with a Shimadzu GC2014C gas chromatography apparatus. Methanol permeability, P_M, was calculated from Eq. (4):

$$P_M = \frac{C_b V_b L}{A C_a t} \quad (4)$$

where C_a and C_b refer to the methanol concentration in feed and permeate at time t, respectively. V_b is the solution volume of the permeate. L and A refer to the thickness and effective area of the swollen membrane, respectively.

3. Results and discussion

3.1. Characterization of crosslinkable SPAEKs

Table 1 lists a series of SPAEK copolymers prepared in this study (**B1**–**B4**) and their fundamental properties. The molar ratio of CBFBS to DFB was set in the range of 1/1–4/1 to achieve the copolymers with high IEC (>2.0 mequiv. g^{-1}). All the copolymers were prepared with high yields and had high intrinsic viscosities ranged from 1.5 to 1.8 dL g^{-1}, indicating the high molecular weights. The IEC values determined by the titration method were about 10% smaller than those of the calculated ones, as often reported in literature.

The chemical structure was identified by ^{1}H NMR and IR spectra. Fig. 2 shows the ^{1}H NMR spectra of **B1** and **B3**. The signal at 8.25 ppm was assigned to the aromatic hydrogen atom H8 at the *ortho* position to the electron-withdrawing –SO_3H group. Comparing the ^{1}H NMR spectra of the copolymers with that of DFB shown in Fig. 1(b), four new peaks at 6.83, 7.32, 7.55, and 7.90 ppm, were assigned to the aromatic hydrogen atoms H2, H1, H4 + H5, and H3 at benzil groups, respectively.

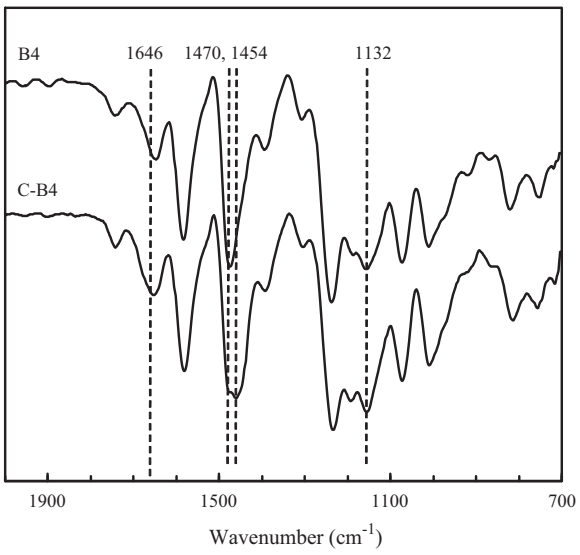

Fig. 3. IR spectra of SPAEK membranes.

Table 2
Solubility properties of SPAEK membranes[a].

Code	DMSO	NMP	DMAc	DMF
B1	++(++)	+(+−)	+(+−)	++(++)
C-B1	+−(+−)	−(+−)	−(+−)	+−(+−)
B2	+(++)	+(++)	++(++)	+(++)
C-B2	+−(+−)	−(+−)	−(+−)	+−(+−)
B3	++(++)	−(+)	+(+)	+(+)
C-B3	−(+−)	−(+−)	−(+−)	−(−)
B4	++(++)	+(++)	++(++)	++(++)
C-B4	−(+−)	−(−)	−(−)	+−(+)

[a] ++, soluble at room temperature; +, soluble at elevated temperature; +−, partially soluble; −, insoluble. The data in parentheses refer to sodium salt form and others refer to proton form.

Integration of ^{1}H NMR signals was used to calculate the sulfonation content (SC) which represents the actual mole percentage of sulfonated unit per average repeat unit in the obtained copolymers. The ratio of the integration value of proton H3–H8 was used for the calculation. The SC determined by the ^{1}H NMR method was in good agreement with the one calculated from the molar feed ratio within the difference of ±1 mol%, which implied that the polymerization was performed completely.

Fig. 3 shows the IR spectrum of **B4**. The absorption bands at 1646 cm^{-1} and 1739 cm^{-1} were assigned to symmetric and asymmetric stretching vibrations of C=O. The symmetric and asymmetric vibration of O=S=O bond of sulfonic acid group appeared at 1010, 1070 and 1150 cm^{-1}. The 1230 cm^{-1} peak was attributed to the vibrations of C–O–C group in aryl ether backbone.

3.2. Crosslinking of SPAEK

Table 1 also lists crosslinked SPAEK membranes (**C-B1**–**C-B4**) and their fundamental properties. The formation of crosslinking was confirmed by IR measurement and also judged by the insolubility of the crosslinked membranes in common aprotic solvents in which the corresponding uncrosslinked membranes were well soluble. Fig. 3 shows the IR spectra of the uncrosslinked and crosslinked membranes (**B4** and **C-B4**, respectively) in proton form. Although the two spectra were similar, the following differences were observed for **C-B4**. The peak appeared at 1182 cm^{-1} was assigned to the characteristic stretching vibration of C–N. Although overlapping with that of phenyl ring (1470 cm^{-1}), the characteristic absorption bands of quinoxaline ring resulted in a strong shoulder peak at 1454 cm^{-1}. In addition, the slightly wider peak at 1646 cm^{-1} for **C-B4** than for **B4** was attributed to the vibration of C=N of quinoxaline ring. These indicated the formation of quinoxaline ring. The characteristic absorption bands of amino group at 3000–3400 cm^{-1} was not detected for **C-B4** in sodium salt form as well as in proton form, indicating the absence of the unreacted diamino-phenyl end-groups. It was confirmed that the crosslinking of SPAEK was performed well with the formation of the quinoxaline cross-linkage.

As listed in Table 1, the titrated IEC values of the crosslinked membranes were about 20% smaller than the calculated ones, whereas those of the uncrosslinked ones were about 10% smaller. This was due to the formation of acid–base complex between sulfonic acid groups and quinoxaline moieties.

3.3. Solubility, thermal and mechanical properties

The solubility properties of SPAEKs are listed in Table 2. The uncrosslinked SPAEKs generally showed good solubility to the polar aprotic solvents such as DMSO, NMP and DMF, both in sodium salt and in proton form. Generally, crosslinking reduces the solubility. The crosslinked SPAEKs in sodium salt form were only partially soluble in polar aprotic solvents even at elevated temperature, indicating the construction of the covalent crosslinking network. After the proton exchange treatment, the crosslinked SPAEK membranes became insoluble in most of the tested polar aprotic solvents. This suggests that the crosslinking network of the crosslinked SPAEK membranes was further improved by the ionic acid–base crosslinkage between sulfonic acid groups and quinoxaline groups.

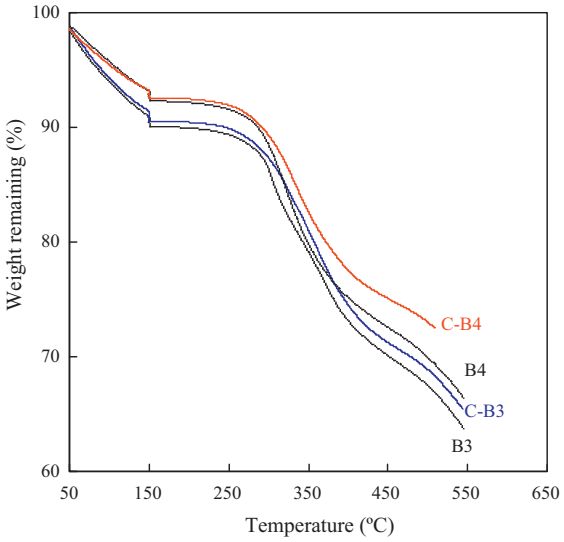

Fig. 4. TGA curves of SPAEK membranes.

The thermal stability of SPAEKs in proton form was examined by TGA. Above 150 °C, the two step degradation profile was observed for all of the membranes, as shown in Fig. 4. The weight loss below 400 °C was attributed to the cleavage of sulfonic acid groups, whereas the weight loss above 500 °C was attributed to the decomposition of polymer backbone. The first decomposition (desulfonation) temperature (T_{ds}) was 284 °C for the uncrosslinked membranes and 295 °C for the crosslinked membranes. The slightly higher T_{ds} for the latter was caused by the acid–base interaction between sulfonic acid groups and quinoxaline groups.

Fig. 5 shows the tensile stress–strain curves of SPAEK membranes. The mechanical property was characterized by Young's modulus (M), maximum stress (S) and elongation at break (E). The data are also listed in Fig. 5. All the SPAEK membranes had much higher Young's modulus, yield point and maximum stress than Nafion 112 (M of 0.24 GPa, S of 40 MPa and E of 380%), and reasonably large elongation at break point, indicating their

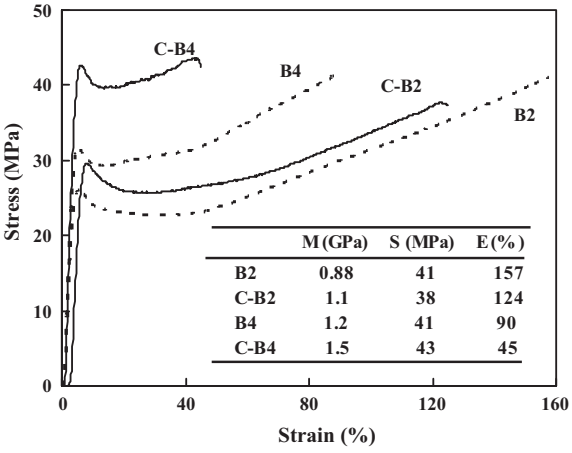

Fig. 5. Tensile stress–strain curves of SPAEK membranes.

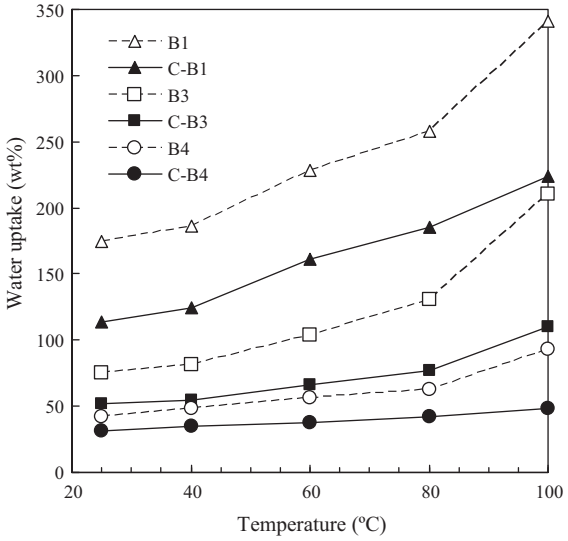

Fig. 6. Temperature dependence of water uptake of SPAEK membranes.

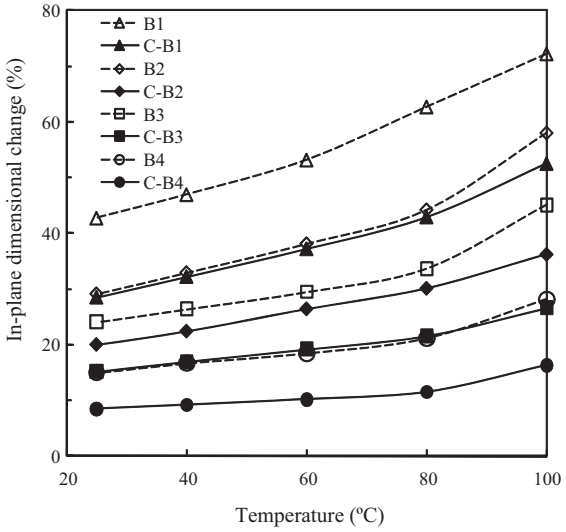

Fig. 7. Temperature dependence of *in-plane* dimensional change of SPAEK membranes.

excellent mechanical properties. Compared to the uncrosslinked membranes (**B2**, **B4**), the corresponding crosslinked ones (**C-B2**, **C-B4**) showed the higher Young's modulus and yield point, but the smaller elongation after the yield point to the break point and the similar maximum stress. This indicates that the crosslinked SPAEK membranes were slightly stiffer than the uncrosslinked ones. All the SPAEK membranes were tough even in the dry state.

3.4. Water uptake and dimensional change

The water uptake of sulfonated polymers mainly depends on the IEC, and has a profound influence on the proton conductivity because sulfonic acid groups need to dissociate for the proton to become mobile and transportable in membrane. So the higher water uptake leads to the higher proton conductivity. However, the excessive water uptake in membrane will result in both the loss of dimensional stability and the dilution of the proton concentration in membrane, which will cause a dimensional mismatch of membrane–electrode assembly and a decrease in the proton conductivity. Therefore, a proper water content level in membrane should be maintained in order to guarantee the dimensional stability and high proton conductivity.

The water uptake data of the uncrosslinked and crosslinked SPAEK membranes at different temperatures are summarized in Table 1 and Fig. 6. With increasing temperature from 25 to 100 °C, the water uptake increased largely especially for the membrane with the higher IEC. Although the crosslinked membranes had the slightly lower calculated IECs than the corresponding uncrosslinked ones, the former displayed the much lower water uptakes than the latter, especially at elevated temperatures. For example, **C-B3** showed reasonably low water uptakes of 52% and 77% at 25 °C and 80 °C, respectively, whereas **B3** showed high values of 75% and 131%, respectively. It is noted that the covalent and ionic crosslinking suppressed the polymer chain relaxation in water, resulting in the reduced water uptake. As the WU significantly depends on the IEC, the comparison of water uptake among membranes with different IECs is often performed in terms of the number of sorbed water molecules per sulfonic acid group (λ). The λ values were calculated using the calculated IEC values, and are listed in Table 1. The λ still increased fairly largely with an increase in IEC. The crosslinked SPAEKs with IEC of 2.02–2.54 mequiv. g^{-1} (**C-B2**–**C-B4**) showed the λ values of 12–20 at 80 °C, which were smaller than those (17–34) of the uncrosslinked SPAEKs with the similar IEC of 2.08–2.61 mequiv. g^{-1}.

Through-plane and *in-plane* membrane dimensional changes at different temperatures were measured and the results are summarized in Table 1 and Fig. 7. The uncrosslinked and crosslinked SPAEK membranes showed the isotropic membrane swelling with $\Delta_{t/l}$ values close to unity. This is similar to the case of Nafion and SPAEs [13(c),17], but different from the case of sulfonated polyimides (SPIs) with the larger *through-plane* dimensional change than the *in-plane* one [10,23]. The dimensional change increased with an increase in temperature and also with an increase in IEC, as similarly observed for the water uptake. Compared to the uncrosslinked membranes, the crosslinked membranes had the much lower dimensional changes. The dimensional changes of **C-B4** were 0.088 and 0.11 at 25 and 80 °C, respectively, which are reasonably low for fuel cell applications. **C-B3** and **B4** showed fairly large dimensional changes of 0.15 and 0.21 at 25 and 80 °C, respectively, whereas the dimensional changes of the other membranes are too large.

The reported values of water uptake, λ and dimensional change Δl_c for Nafion 117 and 1135 membranes were in the range of 19–22 wt%, 12–13 and 0.11–0.12, respectively, at 25 °C and 29–38 wt%, 18–23 and 0.20 0.24 at 80 °C. [18–20,34] The water uptakes based on the volume were 37–43 vol% and 57–75 vol % at 25 and 80 °C, respectively, for Nafion, whereas they were 41 vol % and 55 vol % at 25 and 80 °C, respectively, for **CB-4**. It is noted that the dimensional changes at 80 °C for Nafion membranes were two times larger than that for **C-B4** and comparable to that for **C-B3** and **B4**.

3.5. Oxidative stability

The oxidative stability for peroxide radical attack was investigated by measuring the elapsed time that a membrane became broken after immersing the membrane sample into Fenton's reagent (3 wt% H_2O_2 + 2 ppm $FeSO_4$) at 80 °C. The results are listed in Table 3. The crosslinked SPAEK membranes exhibited more oxidative stability than those of the corresponding uncrosslinked ones. This is attributed to their lower water uptake as well as the covalent and ionic cross-linking.

Table 3
Proton conductivity, oxidative stability and methanol permeability of SPAEK membranes.

Code	σ[a] (mS cm^{-1})		ΔE_a (kJ mol^{-1})	Oxidative stability τ_1[b] (min)	P_M[c] (10^{-6} cm^2 s^{-1})	φ[c] (10^4 S cm^{-3} s)
	25 °C	80 °C				
B1	125	242	11	110	6.1	2.0
C-B1	107	258	14	150	3.0	3.6
B2	98	191	11	130	3.9	2.5
C-B2	81	194	14	205	1.92	4.3
B3	80	165	12	134	2.5	3.2
C-B3	69	170	15	218	1.21	5.8
B4	60	152	15	143	1.32	4.6
C-B4	39	111	18	295	0.55	7.1

[a] In water.
[b] τ_1 refers to the elapsed time that the membranes became broken.
[c] At 32 wt% methanol solution and 25 °C.

3.6. Proton conductivity

The proton conductivity (σ) data are summarized in Table 3 and Fig. 8. The conductivity significantly depended on IEC, water uptake and temperature. The apparent activation energy (ΔE_a) of proton conductivity was evaluated in the temperature range of 25 °C up to 100 °C for **B4** and **C-B4** and up to 80 °C for the other membranes. For the membrane with the higher water uptake, the proton conductivity at 100 °C was more largely deviated downwards from the Arrhenius plot-line. The ΔE_a values of the crosslinked membranes were larger than those of the corresponding uncrosslinked ones. The ΔE_a values (14–18 kJ mol^{-1}) for the present SPAEK membranes except for **B1**–**B3** were comparable to those reported for SPAEs (13–25 kJ mol^{-1}) [18–22,33,34].

At 25 °C, the SPAEK membrane with the higher IEC showed the higher proton conductivity. The conductivities of the crosslinked membranes were about 15% (for **C-B1**–**C-B3**) or 35% (for **C-B4**) smaller than those of the corresponding uncrosslinked ones. At 80 °C, the uncrosslinked membranes with the higher water uptakes (**B1**–**B3**) showed the smaller proton conductivities than the corresponding crosslinked ones. This was apparently due to the smaller ΔE_a (11–12 kJ mol^{-1}) for **B1**–**B3**. The increased water uptake at the higher temperature causes the dual effects on the proton conductivity, namely the positive effect of promotion of proton migration and the negative effect of dilution of sulfonic acid concentration. For the membrane with an extremely high water uptake, the latter negative effect may not be negligible compared to the former positive one.

For comparison, the water uptakes and proton conductivities in water at 80 °C for representative SPAEs reported in literature are listed in Table 4. In general, SPAEs are copolymers composed of sulfonated hydrophilic units and nonsulfonated hydrophobic units, and the latter units are required to control the IEC and water uptake to suitable levels. The present uncrosslinked membrane (**B4**) showed the larger (or similar) proton conductivity with the lower water uptake at 80 °C, compared to the

Table 4
Comparison of water uptake, σ, P_M and φ among PEMs.

Code	Membrane	IEC (mequiv. g^{-1})	WU[a] (%)	σ[b] (mS cm^{-1})		P_M[c] (conc./temp.) (10^{-6} cm^2 s^{-1})	10^{-4} φ (S cm^{-3} s)	Refs.
				25 °C	80 °C			
B4	SPAEK (B4)	2.08	63	60	152	1.32 (32/25)	4.6	This work
C-B4	Cross-SPAEK (C-B4)	2.02	42	39	111	0.55 (32/25)	7.1	This work
R1	SPAEK-6F-50	1.64	68		80			[20]
R2	SPAEK-6F-60	1.93	157		110			[20]
R3	COOH-SPAEK-3	1.13	62	36	120	0.38 (3.2/25)	9.3	[34]
R4	COOH-SPAEK-4	1.35	169	73	160	0.86 (3.2/25)	8.5	[34]
R5	Cross-SPAEK6d	1.68	39	(23)	32			[32]
R6	Cross-SPAEK6e	2.19	50	(32)	41			[32]
R7	Cross-SPEEK-55-10 min	1.70	47	22	59	0.14 (3.2/25)	15.7	[31]
R8	Me-6F-SPEEK-80	1.71	76	32	172	0.19 (8.0/30)	16.8	[22]
R9	Ph-6FA-SPEEK-80	1.75	81	27	109	0.53 (8.0/30)	5.1	[22]
R11	SPEEKK-3	1.69	24	32	80	0.50 (100/25)	6.4	[21]
R12	SPEEKK-4	1.98	30	40	100	0.56 (100/25)	7.1	[21]
R13	Me-SPEEKK	1.78	49	(33)	154	0.23 (8.0/30)	14.5	[22]
R14	Ph-SPEEKK	1.82	51	(38)	151	0.33 (8.0/30)	11.5	[22]
R21	SPAES(BPSH-40)	1.72		100		0.81 (6.5/25)	12.3	[13(a)]
R22	SPAES(6FCN-35)	1.32		80		0.87 (6.5/25)	9.2	[13(b)]
R23	SPAES(BPSH40-0)	1.59	43	(102)	270	1.6 (32/30)	6.4	[33]
R24	Cross-SPAES(BPSH40-10)	1.63	23	(93)	245	0.60 (32/30)	15.5	[33]
R25	Cross-SPAES(BPSH40-30)	1.61	21	(92)	240	0.41 (32/30)	22	[33]
R26	SC-SPAE80	1.52	23	10	34	0.16 (48/25)	6.1	[18]
R27	S2-PAES-50	1.80	37	(29)	88	0.174(8.0/30)	16.7	[19(a)]
R28	SPAE-0.64	1.14	26	(52)	101	0.29 (8.0/30)	17.6	[19(b)]
R29	Cross-SPSSF-50	1.34	80	(65)		0.43 (8.9/30)	15	[15]
R31	SPI(NTDA/2,2′-BSPB)	2.02		(52)		0.34 (10/30)	15	[35]
R32	SPI(NTDA/BAPBDS)	1.89		(72)		0.75(10/30)	9.6	[35]
	Nafion 112	0.91		(100)		2.4 (10/30)	4.2	[35]
	Nafion 117	0.91	29	57	125	1.6(8.0/30)	3.7	[19(b)]

[a] Water uptake at 80 °C.
[b] In water at 25 (or 30) and 80 °C.
[c] At the conditions of methanol concentration (wt%) and temperature (°C) given in parentheses.

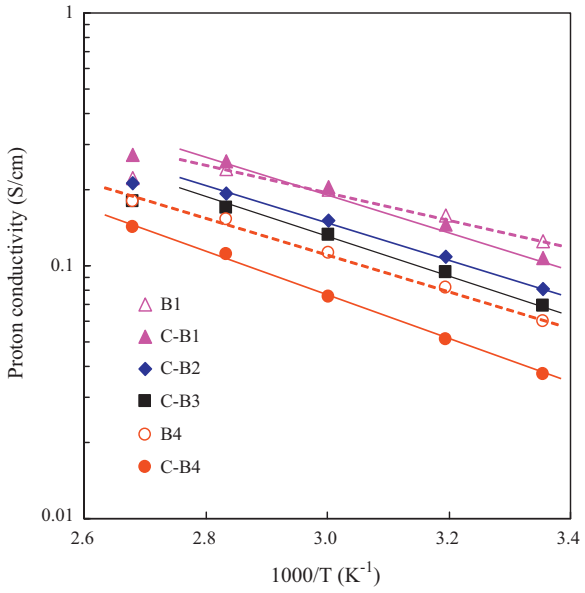

Fig. 8. Temperature dependence of proton conductivity of SPAEK membranes.

other uncrosslinked SPAEK membranes (R1–R4 and R8–R9), indicating that the introduction of benzil groups in nonsulfonated hydrophobic units was useful to achieve the better balance of water uptake and conductivity. The SPEEKK membranes (R11–R14) have been reported to have the reasonably high proton conductivities (80–154 mS cm^{-1}) with the relatively low water uptakes (24–51%).

The reported values of water uptake, size change Δl_c and proton conductivity in water at 80 °C for Nafion 117 and 1135 membranes were in the range of 57–75 vol%, 0.20–0.24 and 83–125 mS cm^{-1}, respectively. [18–20,34] The corresponding values for the present crosslinked membrane (**C-B4**) were 55 vol%, 0.11 and 111 mS cm^{-1}, respectively. It is noted that **C-B4** showed the much smaller size change and the comparable proton conductivity compared to Nafion membranes. **C-B4** showed the 2–3 times larger conductivity in spite of the comparable or lower water uptake than the crosslinked SPAEK membranes (R5–R7). On the other hand, the crosslinked SPAES membranes (R24–R25) have been reported to have the much larger conductivities (245 mS cm^{-1}) with the much lower water uptakes (23%).

3.7. Methanol permeability

The methanol permeability (P_M) and the ratio of proton conductivity to methanol permeability (φ), which is an effective parameter to evaluate the performance of membrane in a DMFC system, are summarized in Table 3. For the uncrosslinked PAEK membranes, with decreasing IEC, the methanol permeability decreased more largely than the proton conductivity. **B4** with the lowest IEC (2.08 mequiv. g^{-1}) showed the lowest P_M of 1.32×10^{-6} cm^2 s^{-1} and the largest φ of 4.6×10^4 S cm^{-3} s. The crosslinked membranes showed the more than two times lower methanol permeabilities and the 55–80% larger φ values than the corresponding uncrosslinked ones. **C-B4** showed the lowest P_M of 0.55×10^{-6} cm^2 s^{-1} and the largest φ of 7.1×10^4 S cm^{-3} s among the present SPAEK membranes. This performance was fairly high, taking the high feed methanol concentration (32 wt%) into account.

For comparison, the σ, P_M and φ values at 25 °C (or 30 °C) for representative SPAEs reported in literature are listed in Table 4. As the feed concentration of methanol was different from literature to literature, the rough comparison among the PEMs is preferable. The φ value of the present crosslinked membrane (**C-B4**) was comparable to those of some reported membranes, but many membranes have been reported to have the high φ values of more than 10×10^4 S cm^{-3} s.

In order to clearly investigate the effects of the crosslinking via formation of quinoxaline groups on the water uptake, membrane swelling and proton conductivity, the IECs of the present SPAEK membranes were limited to be higher than 2.0 mequiv. g^{-1}. As can be seen in Table 4 and also from our recent studies on DMFC [36], the PEMs with lower IECs of less than 1.9 mequiv. g^{-1} seems to be preferable to DMFC at mediate temperatures. The further study is necessary to make both the composition of the crosslinkable SPAEK and the crosslinking conditions most suitable to DMFC application.

4. Conclusions

Crosslinked SPAEK membranes were successfully synthesized by the cyclocondensation reaction of the benzil moieties in polymer chain with 3,3′-diaminobenzidine to form quinoxaline groups acting as covalent and acid–base ionic crosslinking. The crosslinked SPAEK membranes became insoluble in most of the tested polar aprotic solvents, and showed the high mechanical properties and the isotropic membrane swelling. They showed the lower water uptake, lower dimensional change, lower methanol permeability and higher oxidative stability than the corresponding uncrosslinked membranes, with keeping the reasonably high proton conductivity. **C-B4** showed a reasonably high proton conductivity of 111 mS cm^{-1} with a low water uptake of 42 wt% at 80 °C. **C-B4** also showed the lowest P_M of 0.55×10^{-6} cm^2 s^{-1} and the largest φ of 7.1×10^4 S cm^{-3} s for 32 wt% methanol solution at 25 °C among the present SPAEK membranes. The crosslinked SPAEK membranes have the higher potential as PEMs by making both their composition and the crosslinking conditions most suitable to PEFC and DMFC applications.

Acknowledgements

The authors would like to thank the Key Technologies R&D Program of Shaanxi Province (no. 2009K06-08), the Fundamental Research Funds for the Central Universities (no. GK200902002), the Scientific Research Foundation for Returned Scholars, Ministry of Education, and the Youth Foundation of School of Chemistry and Materials Science, Shaanxi Normal University for financial support of this work.

References

[1] O. Savadoga, J. New Mater. Electrochem. Syst. 1 (1998) 47–66.
[2] K.A. Mauritz, R.B. Moore, Chem. Rev. 104 (2004) 4535–4585.
[3] V. Mehta, J.S. Cooper, J. Power Sources 114 (2003) 32–53.
[4] M. Rikukawa, K. Sanui, Prog. Polym. Sci. 25 (2000) 1463–1502.
[5] J.A. Kerres, J. Membr. Sci. 185 (2001) 3–27.
[6] K.D. Kreuer, J. Membr. Sci. 185 (2001) 29–39.
[7] J. Roziere, D.J. Jones, Annu. Rev. Mater. Res. 33 (2003) 503–555.
[8] M.A. Hickner, H. Ghassemi, Y.S. Kim, B.R. Einsla, J.E. McGrath, Chem. Rev. 104 (2004) 4587–4612.
[9] A.L. Rusanov, D. Likhatchev, P.V. Kostoglodov, K. Mullen, M. Klapper, Adv. Polym. Sci. 179 (2005) 83–134.
[10] Y. Yin, O. Yamada, K. Tanaka, K. Okamoto, Polym. J. 38 (2006) 197–219.
[11] C. Marestin, G. Gebel, O. Diat, R. Mercier, Adv. Polym. Sci. 216 (2008) 185–258.
[12] K. Goto, I. Rozhanskii, Y. Yamakawa, T. Otsuki, Y. Naito, Polym. J. 41 (2009) 95–104.
[13] (a) Y.S. Kim, M.J. Sumner, W.L. Harrison, J.S. Riffle, J.E. McGrath, B.S. Pivovar, J. Electrochem. Soc. 151 (2004) A2150–A2156;
(b) H. Ghassemi, J.E. McGrath, T.A. Zawodzinski Jr., Polymer 47 (2006) 4132–4139;
(c) H. Lee, A. Roy, O. Lane, M. Lee, J.E. McGrath, J. Polym. Sci. Part A: Polym. Chem. 48 (2010) 214–222.
[14] (a) H.S. Lee, A. Badami, A. Roy, J.E. McGrath, J. Polym. Sci. Part A: Polym. Chem. 45 (2007) 4879–4890;
(b) M.L. Einsla, Y.S. Kim, M. Hawley, H.S. Lee, J.E. McGrath, B. Liu, M.D. Guiver, B.S. Pivovar, Chem. Mater. 20 (2008) 5636–5642.

[15] (a) K. Miyatake, Y. Chikashige, E. Higuchi, M. Watanabe, J. Am. Chem. Soc. 129 (2007) 3879–3887;
(b) B. Bae, T. Yoda, K. Miyatake, H. Uchida, M. Watanabe, Angew. Chem. Int. Ed. 49 (2010) 317–320.
[16] T. Yamaguchi, H. Zhou, S. Nakazawa, N. Hara, Adv. Mater. 19 (2007) 592–596.
[17] (a) K. Nakabayashi, K. Matsumoto, M. Ueda, J. Polym. Sci. Part A: Polym. Chem. 46 (2008) 3947–3957;
(b) K. Matsumoto, T. Higashihara, M. Ueda, Macromolecules 42 (2009) 1161–1166.
[18] J. Pang, H. Zhang, X. Li, Z. Jiang, Macromolecules 40 (2007) 9435–9442.
[19] (a) D.S. Kim, G.P. Robertson, M.D. Guiver, Macromolecules 41 (2008) 2126–2134;
(b) D.S. Kim, G.P. Robertson, Y.S. Kim, M.D. Guiver, Macromolecules 42 (2009) 957–963.
[20] P.X. Xing, G.P. Robertson, M.D. Guiver, S.D. Mikhailenko, S. Kaliaguine, Macromolecules 37 (2004) 7960–7967.
[21] X.F. Li, C.J. Zhao, H. Lu, Z. Wang, H. Na, Polymer 46 (2005) 5820–5827.
[22] B. Liu, G. Robertson, D.S. Kim, M.D. Guiver, W. Hu, Z. Jiang, Macromolecules 40 (2007) 1934–1944.
[23] (a) X. Guo, J. Fang, T. Watari, K. Tanaka, H. Kita, K. Okamoto, Macromolecules 35 (2002) 6707–6713;
(b) Y. Yin, O. Yamada, S. Hayashi, K. Tanaka, H. Kita, K. Okamoto, J. Polym. Sci.: Polym. Chem. 44 (2006) 3751–3762;
(c) H. Bi, S. Chen, X. Chen, K. Chen, N. Endo, M. Higa, K. Okamoto, L. Wang, Macromol. Rapid Commun. 30 (2009) 1852–1856;
(d) K. Yaguchi, K. Chen, N. Endo, M. Higa, K. Okamoto, J. Power Sources 195 (2010) 4676–4684;
(e) K. Okamoto, K. Yaguchi, H. Yamamoto, K. Chen, N. Endo, M. Higa, H. Kita, J. Power Sources 195 (2010) 5856–5861.
[24] (a) N. Asano, M. Aoki, S. Suzuki, K. Miyatake, H. Uchida, M. Watanabe, J. Am. Chem. Soc. 128 (2006) 1762–1770;
(b) A. Kabasawa, J. Saito, H. Yano, K. Miyatake, H. Uchida, M. Watanabe, Electrochim. Acta 54 (2009) 1076–1082.
[25] Z. Qiu, S. Wu, Z. Li, S. Zhang, W. Xing, C. Liu, Macromolecules 39 (2006) 6425–6432.
[26] (a) J. Kerres, A. Ullrich, F. Meier, T. Haring, Solid State Ionics 125 (1999) 243–249;
(b) J. Kerres, A. Ullrich, T. Haring, M. Baldauf, U. Gebhardt, W. Preidel, J. New Mater. Electrochem. Syst. 3 (2000) 229–239.
[27] J. Kerres, W. Zhang, T. Haering, J. New Mater. Electrochem. Syst. 7 (2004) 299–309.
[28] (a) S.D. Mikhailenko, K.P. Wang, S. Kaliaguine, P.X. Xing, G.P. Robertson, M.D. Guiver, J. Membr. Sci. 233 (2004) 93–99;
(b) S.D. Mikhailenko, G.P. Robertson, M.D. Guiver, S. Kaliaguine, J. Membr. Sci. 285 (2006) 306–316.
[29] S. Gu, G. He, X. Wu, Y. Guo, H. Liu, L. Peng, G. Xiao, J. Membr. Sci. 312 (2008) 48–58.
[30] (a) J. Fang, F. Zhai, X. Guo, H. Xu, K. Okamoto, J. Mater. Chem. 17 (2007) 1102–1108;
(b) C. Zhang, X. Guo, J. Fang, H. Xu, M. Yuan, B. Chen, J. Power Sources 170 (2007) 42–45.
[31] S. Zhong, X. Cui, H. Cai, T. Fu, C. Zhao, H. Na, J. Power Sources 164 (2007) 65–72.
[32] F.C. Ding, S.J. Wang, M. Xiao, X.H. Li, Y.Z. Meng, J. Power Sources 170 (2007) 20–27.
[33] S. Feng, Y. Shang, X. Xie, Y. Wang, J. Xu, J. Membr. Sci. 335 (2009) 13–20.
[34] Y. Zhang, Z. Cui, C. Zhao, K. Shao, H. Li, T. Fua, H. Na, W. Xing, J. Power Sources 191 (2009) 253–258.
[35] K. Okamoto, Y. Yin, O. yamada, M.N. Islam, T. Honda, T. Mishima, Y. Suto, K. Tanaka, H. Kita, J. Membr. Sci. 258 (2005) 115–122.
[36] (a) Z. Hu, T. Ogou, M. Yoshino, O. Yamada, H. Kita, K. Okamoto, J. Power Sources 194 (2009) 674–682;
(b) K. Chen, Z. Hu, N. Endo, J. Fang, M. Higa, K. Okamoto, J. Membr. Sci. 351 (2010) 214–221.